# Some analytical results for toroidal magnetic field coils with elongated minor cross-sections

J. Raeder

IPP 4/141 September 1976

MAX-PLANCK-INSTITUT FÜR PLASMAPHYSIK

8046 GARCHING BEI MÜNCHEN

**MAX-PLANCK-INSTITUT FÜR PLASMAPHYSIK**

**GARCHING BEI MÜNCHEN**

# Some analytical results for toroidal magnetic field coils with elongated minor cross-sections

J. Raeder

IPP 4/141 September 1976

*Die nachstehende Arbeit wurde im Rahmen des Vertrages zwischen dem Max-Planck-Institut für Plasmaphysik und der Europäischen Atomgemeinschaft über die Zusammenarbeit auf dem Gebiete der Plasmaphysik durchgeführt.*

IPP 4/141

# Some analytical results for toroidal magnetic field coils with elongated minor cross-sections.

J. Raeder

September 1976


## Abstract

The problem of determining the shape of a flexible current filament forming part of an ideal toroidal magnetic field coil is solved in a virtually analytical form. Analytical formulae for characteristic coil dimensions, stored magnetic energies, inductances and forces are derived for the so-called D-coils.

The analytically calculated inductances of ideal D-coils are compared with numerically calculated ones for the case of finite numbers of D-shaped current filaments.

Finally, the magnetic energies stored in ideal rectangular, elliptic and D-coils are compared.

## 1. Introduction

Toroidal magnetic field coils with elongated minor cross-sections have gained interest for several reasons such as:

- The problem of finding coils which are only subject to tensile forces has two principal solutions. One of them is the so-called D-coil, which is elongated in the direction of the main torus axis.

- Fusion devices with axisymmetric divertors of the double null type need space for the divertor chambers above and below the plasma ring.

- There are some indications that Tokamak plasmas with elongated minor cross-sections will offer the chance of attaining higher values of the plasma ß than are possible with circular cross-sections.

Because of this interest this paper presents information on elongated coils in a virtually analytical form, thus providing simple relations for basic comparisons and scalings.

## 2. Ideal magnetic field coils in pure tension

We shall treat the case of an ideal toroidal field produced by coils which are subject to pure tension. By "ideal" we mean that we disregard the deviations from the 1/r-variation of the field produced by the finite number and size of the coils. The coils themselves are treated as infinitely thin current filaments.

### 2.1 Calculation of the coil contour

A current filament is subject to pure tension if the magnetic force $F_m$ acting on any length element ds with

radius of curvature $\rho_c$ is just balanced by the tensile forces T. This situation is visualized by Fig. 1 and 2.

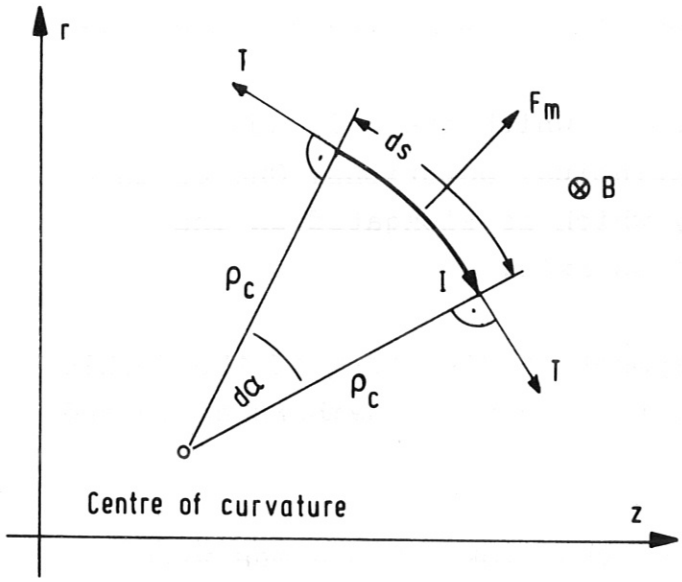


Fig. 1

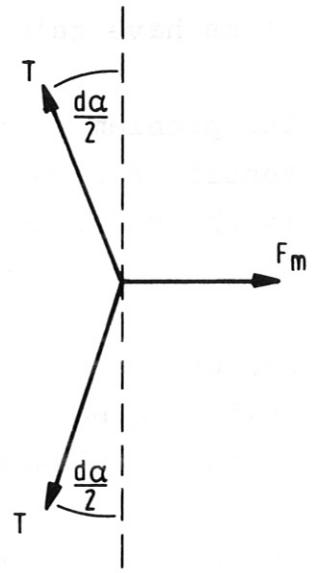


Fig. 2

In the following we restrict ourselves to the case of an ideal toroidal magnetic field, the induction of which varies as

$$B(r) = \frac{r_f}{r} B(r_f) \tag{1}$$

(r = distance from the main torus axis, $r_f$ = arbitrary reference radius).

From Fig. (2) we read

$$T\, d\alpha = F_m \,. \tag{2}$$

With

$$F_m = \frac{1}{2} I B(r)\, ds \tag{3}$$

we get from (2)

$$\frac{d\alpha}{ds} = \frac{1}{2} \cdot \frac{I B(r)}{T} \,. \tag{4}$$

By using the definition of the radius of curvature $\rho_c$ of a plane curve

$$\rho_c = \frac{ds}{d\alpha} \tag{5}$$

we get from (4)

$$\rho_c = \frac{2T}{IB(r)} . \tag{6}$$

If we set the reference ratius $r_f$ equal to $r_i$ (see Fig. 3), we find from (1) and (6) that

$$\rho_c = k r \tag{7}$$

with

$$k = \frac{2T}{IB(r_i) r_i} . \tag{8}$$

If we use the formula

$$\frac{1}{\rho_c} = \frac{d^2r/dz^2}{[1+(dr/dz)^2]^{3/2}} \tag{9}$$

together with (7), we find the well known differential equation for the contour of a filament in pure tension for the case of an ideal toroidal magnetic field [1]:

$$r \frac{d^2r}{dz^2} = \frac{1}{k}\left[1+\left(\frac{dr}{dz}\right)^2\right]^{3/2} . \tag{10}$$

The solution of (10) gives a cycloid-type curve as shown in Fig. 3. Because we aim at a parameter representation of the contour, we shall proceed from (7) in a way different from that in [1]. From Fig. 4 we read the following relationships:

$$dr = ds \cdot \sin\alpha , \tag{11}$$

$$dz = ds \cdot \cos\alpha , \tag{12}$$

where ds is the length element of the contour to be determined.

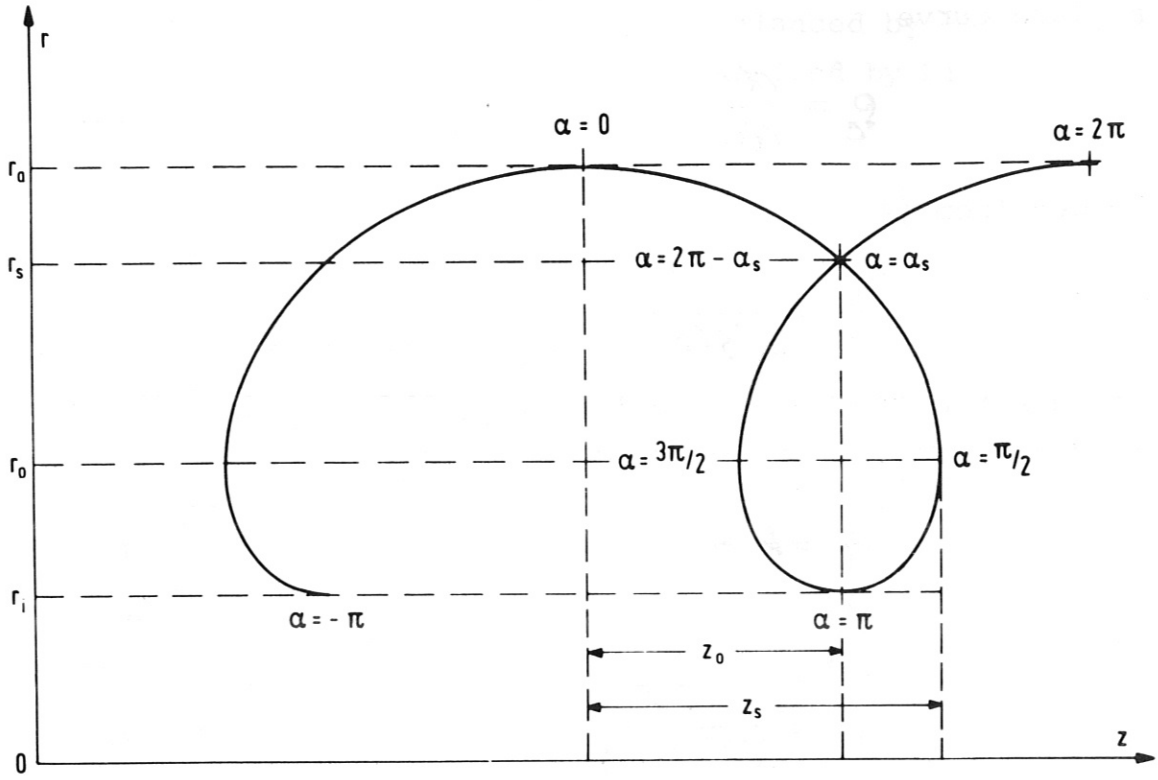


Fig. 3

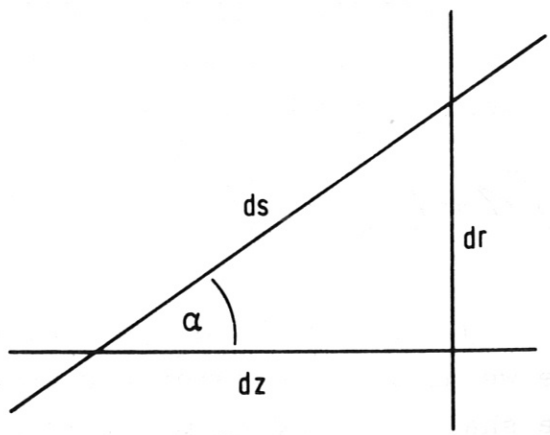


Fig. 4

Equations (5), (7) and (11) together yield

$$\frac{dr}{r} = k \sin\alpha . d\alpha \,, \tag{13}$$

which can readily be integrated to give

$$r = r_a e^{-k} e^{k\cos\alpha} \,. \tag{14}$$

In deriving (14), we have used the initial condition

$$r(\alpha=0) = r_a \,. \tag{15}$$

The parameter $\alpha$, which varies along the contour, is the angle between the tangent of the contour and the z-axis. Because r is an even function of $\alpha$, we can replace $-\alpha$ by $\alpha$. Points on the contour corresponding to characteristic values of $\alpha$ thus defined are marked in Fig. 3.

From Fig. 3 we read

$$r_0 = r(\alpha=\pi/2) = r_a e^{-k} \,, \tag{16}$$

$$r_i = r(\alpha=\pi) = r_a e^{-2k} \,. \tag{17}$$

From (16) and (17) we reproduce the well known formulae

$$r_0 = (r_a r_i)^{1/2} \,, \tag{18}$$

$$k = \frac{1}{2} \ln(r_a/r_i) \,. \tag{19}$$

From eqs. (5), (7), and (12) we find

$$dz = k r \cos\alpha . d\alpha \,. \tag{20}$$

By inserting (14) in (20) we arrive at the differential equation for $z(\alpha)$:

$$\frac{dz}{d\alpha} = r_a k e^{-k} e^{k\cos\alpha} \cos\alpha \,. \tag{21}$$

With the initial condition

$$z(\alpha=0)=0 \tag{22}$$

we get from (21)

$$z(\alpha)=r_a k e^{-k}\int_0^{\alpha} e^{k\cos\alpha'}\cos\alpha'\,.\,d\alpha'. \tag{23}$$

Because of

$$\int_0^{\tilde{\pi}} e^{k\cos\alpha'}\cos(n\alpha')\,.\,d\alpha'=\tilde{\pi}\,I_n(k) \tag{24}$$

($I_n$ = modified Bessel function of the first kind and order n) we get for $z_o$ and $s_o$ (the half-length of the curved part of the contour)

$$z_0=z(\alpha=\tilde{\pi})=\tilde{\pi}\,r_a k e^{-k}I_1(k)=\tilde{\pi}\,r_0 k I_1(k) \tag{24}$$

and $$s_0=s(\alpha=\tilde{\pi})=\tilde{\pi}\,r_a k e^{-k}I_0(k)=\tilde{\pi}\,r_0 k I_0(k). \tag{25}$$

For many applications it is adequate to give $z(\alpha)$, $r(\alpha)$, $z_o$ and $s_o$ in terms of k and the inner radius $r_i$:

$$z(\alpha)=r_i k e^{k}\int_0^{\alpha} e^{k\cos\alpha'}\cos\alpha'\,.\,d\alpha', \tag{26}$$

$$r(\alpha)=r_i e^{k} e^{k\cos\alpha}, \tag{27}$$

$$z_0=\tilde{\pi}\,r_i k e^{k}I_1(k), \tag{28}$$

$$s_0=\tilde{\pi}\,r_i k e^{k}I_0(k). \tag{29}$$

The functions $z_o/r_i$ and $s_o/r_i$ vs. $r_a/r_i$ are shown in Fig. 5.

The integral in (26) can very easily be calculated numerically because the integrand does not exhibit any singularities. A term by term integration of any absolutely convergent series expansion of exp(k cosα) is easily possible.

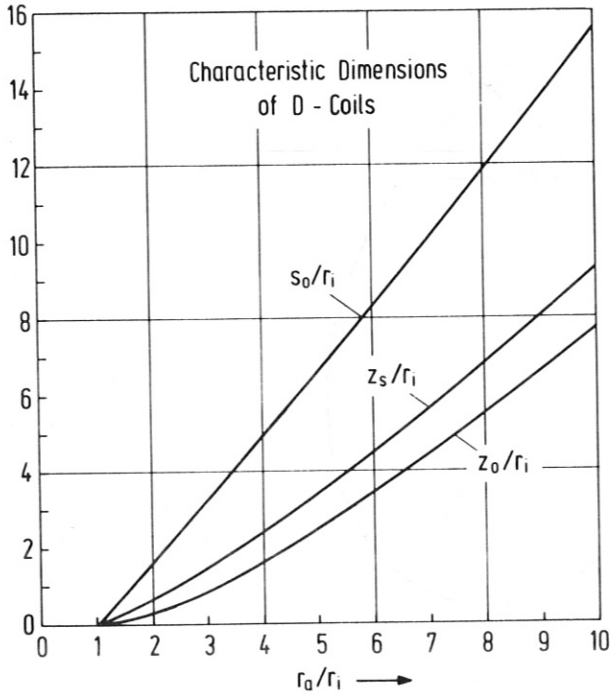


Fig. 5

## 2.2 Different types of coils in pure tension

If we connect the points $\alpha = \pi$ and $\alpha = -\pi$ (see Fig. 3) by a straight line, we get the contour of the so-called D-coil. Obviously, this coil is in pure tension only in its curved parts. The straight part is subject to both tension and lateral forces directed radially inward.

A possibility of getting a closed coil which is in pure tension in all its parts is presented by choosing the drop-shaped loop between $\alpha = \alpha_s$ and $\alpha = 2\pi - \alpha_s$ (see Fig. 3). Because this coil contains the point where two branches of the contour cross over, there exists a sharp edge. To avoid this one may cut the edge by a straight line parallel to the z-axis as shown in Fig. 6.

Obviously this straight portion again is subject to lateral forces directed radially inward. These forces result from the tension in the curved parts and from the magnetic field acting on the current in the straight part.

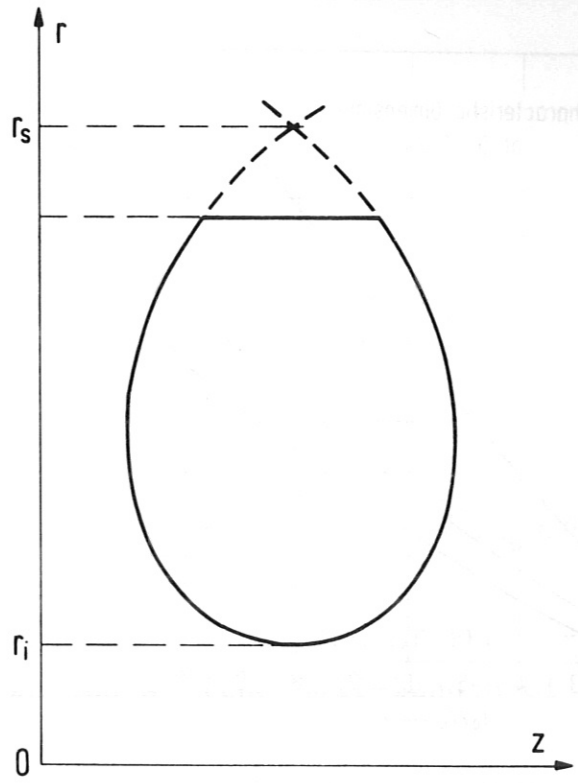


Fig. 6

Figures 7 and 8 show D-coils and drop-shaped coils respectively. The curves are normalized to get the same radial extent for all coils. This makes it possible to compare the shapes of coils corresponding to different values of $r_a/r_i$. The shape of one coil is completely determined by the value of k chosen.

With values of k approaching zero the D-coils and the drop-shaped coils approach circles. This can be seen from, for instance, (26) and (27) if we calculate the limiting values of z and r for $k \to 0$:

$$\lim_{k \to 0} z = r_0 k \sin\alpha \,, \tag{30}$$

$$\lim_{k \to 0} r = r_0 (1 + k \cos\alpha) \,. \tag{31}$$

Equations (30) and (31) describe a circle with radius $kr_0$ centered at z = o, r = $r_0$. This limiting case is only of

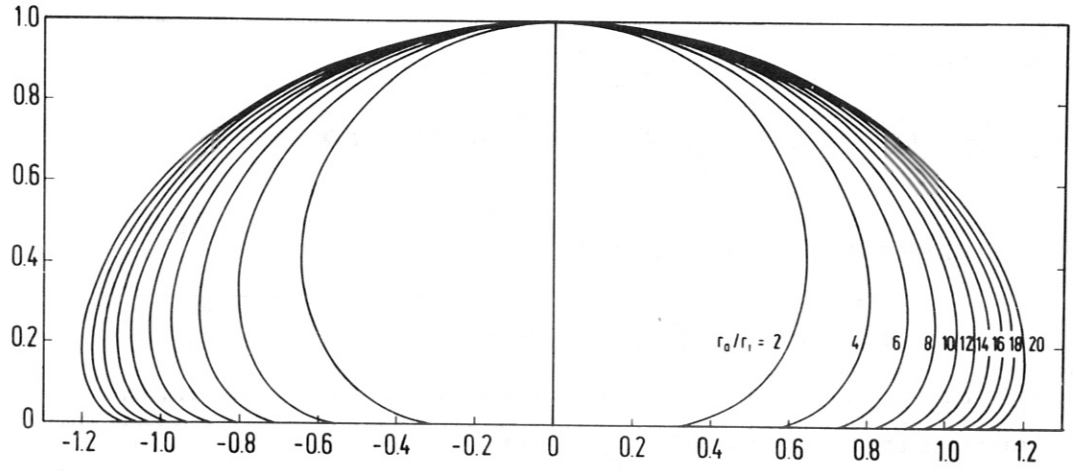
1.0
0.8
0.6
0.4
0.2
0
-1.2
-1.0
-0.8
-0.6
-0.4
-0.2
0
0.2
0.4
0.6
0.8
1.0
1.2
$r_a/r_i$ = 2
4
6
8
10
12
14
16
18
20

Fig. 7

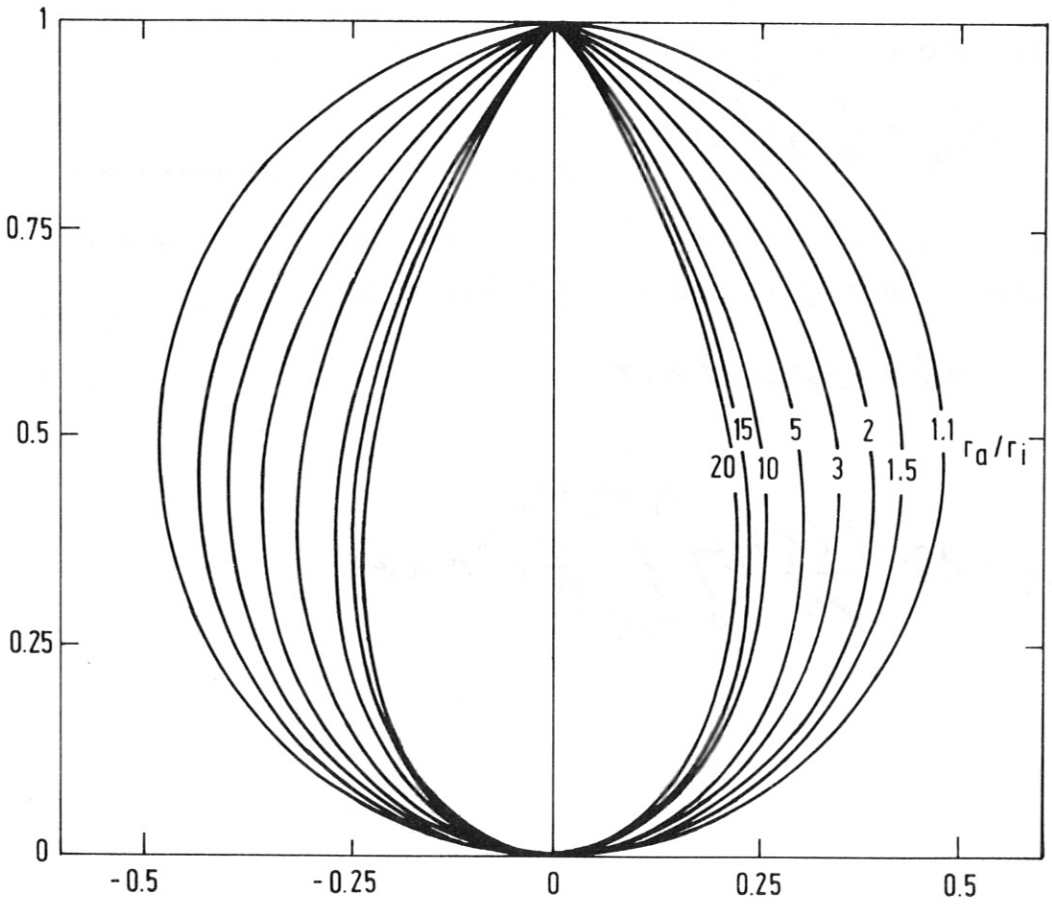
1
0.75
0.5
0.25
0
-0.5
-0.25
0
0.25
0.5
15
5
2
1.1
20
10
3
1.5
$r_a/r_i$

Fig. 8

academic interest because $k \rightarrow 0$ corresponds to a vanishing difference between the outer and inner radii $r_a$ and $r_i$.

The half-height $z_s$ of a D-coil is given by

$$z_s = z(\alpha = \hat{\iota}/2) = r_i k \int_0^k e^{\hat{\iota}/2 \, k \cos\alpha'} \cos\alpha' \, d\alpha' . \tag{32}$$

Figure 5 shows $z_s/r_i$ vs. $r_a/r_i$.

$z_s/r_i$ and $z_o/r_i$ approach zero for $r_a/r_i \longrightarrow 1$, which corresponds to the limiting case of a circular contour. With increasing values of $r_a/r_i$ the two curves diverge which corresponds to an increasing degree of elongation of the contour in the z-direction. Coils envisaged today are in the vicinity of $r_a/r_i = 5$.

## 2.3 The stored magnetic energy of D-coils

The magnetic energy stored in an air coil is given by

$$E_m = \int_V \frac{B^2}{2\mu_0} \, dV . \tag{33}$$

For our idealized case the volume V is that swept by the D-contour rotating around the z-axis. With

$$dV = 2\hat{\iota} \, r \, dr \, dz \tag{34}$$

we get

$$E_{m,T} = 2\hat{\iota} \, \frac{B^2(r_i)}{\mu_0} r_i^2 \int_0^{z_s} \int_{r_{ci}(z)}^{r_{ca}(z)} \frac{1}{r} \, dr \, dz \tag{35}$$

($r_{ca}$ is the branch of the contour between $\alpha = 0$ and $\alpha = \pi/2$, $r_{ci}$ is that part of the contour beyond $\alpha = \pi/2$; see Fig. 3). The factor 2 in front of the integral (35) originates from restricting the interval of integration to $0 \leq z \leq z_s$, which is possible because of symmetry.

By integrating (35) with respect to r we get

$$E_{m,D} = 4\pi \frac{B^2(r_i)}{2\mu_0} r_i^2 k \int_0^{z_s} \ln \frac{r_{ca}}{r_{ci}} \, dz . \qquad (36)$$

The integration in (36) can be performed by using (27) and yields

$$E_{m,D} = 4\pi^2 k e^k [k I_0(k) + (k-1) I_1(k)] \frac{B^2(r_i)}{2\mu_0} r_i^3 . \qquad (37)$$

This expression can be compared with that for a toroidal coil with circular cross-section:

$$E_{m,c} = 4\pi^2 \cdot 2 e^k (\sinh k/2)^2 \frac{B^2(r_i)}{2\mu_0} r_i^3 . \qquad (38)$$

The ratio of the magnetic energies stored in a D-coil and in a circular coil for identical values of k, $r_i$ and $B(r_i)$ is

$$\frac{E_{m,D}}{E_{m,c}} = \frac{k[k I_0(k) + (k-1) I_1(k)}{2 (\sinh k/2)^2} . \qquad (39)$$

Figure 9 shows $E_{m,D}/E_{m,c}$ vs. $r_a/r_i$ and the aspect ratio $A_m$ (see section 4).

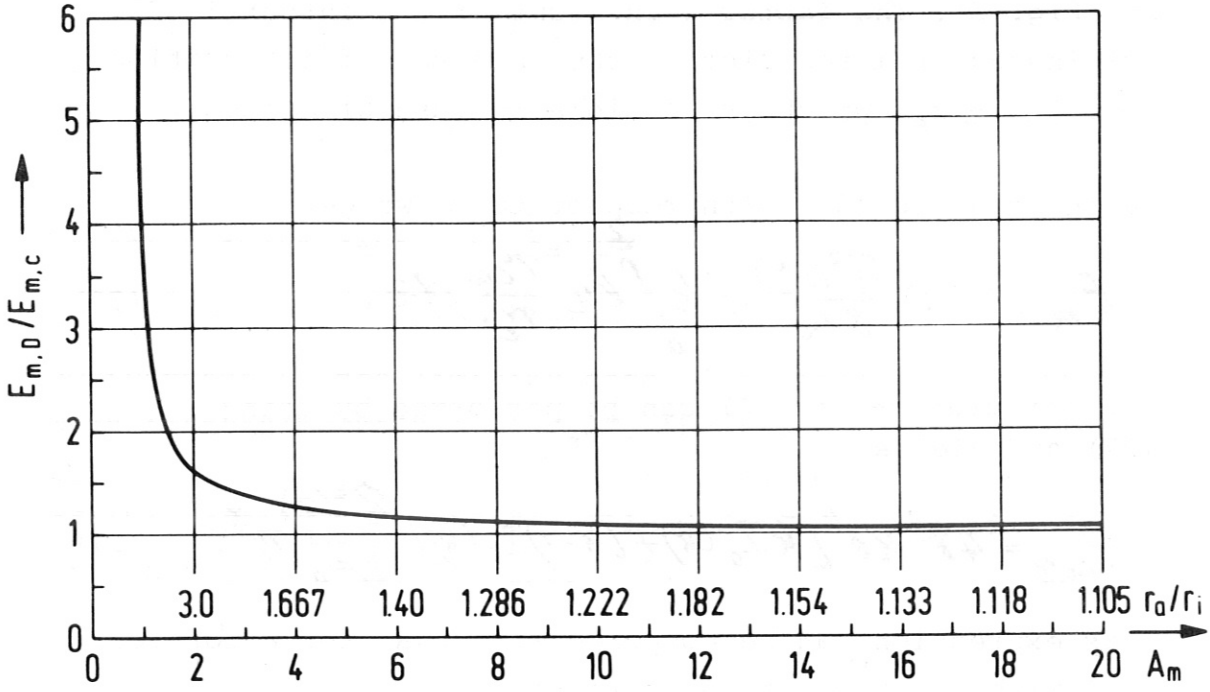


Fig. 9

## 2.4 The inductance of D-coils

We treat the case of N D-shaped turns carrying the current I which are arranged toroidally. In the ideal case we have

$$B(r_i) = \frac{\mu_0 N I}{2\pi r_i} \quad . \tag{40}$$

The inductance $L_D$ is related to the stored magnetic energy $E_{mD}$ by

$$L_D = \frac{2 E_{mD}}{I^2} \quad . \tag{41}$$

By inserting $E_{mD}$ from (37) and I from (40) in (41) we get

$$L_D = N^2 \mu_0 k e^k [k I_0(k) + (k-1) I_1(k)] r_i . \qquad (42)$$

For equal numbers of ampere-turns the ratio of the inductances of D-coils and circular coils is the same as the ratio of the magnetic energies according to (39).

## 2.5 Forces and stresses pertaining to D-coils

The lateral force $K_r$ which acts radially inward on one D-turn is given by

$$K_r = \frac{1}{2} I B(r_i) 2 z_0 . \qquad (43)$$

By inserting I from (40) in (43) we get

$$K_r = \frac{1}{N} 4 \tilde{i} r_i z_0 \frac{B^2(r_i)}{2\mu_0} . \qquad (44)$$

Insertion of $z_0$ from (28) in (44) yields

$$K_r = \frac{1}{N} 4 \tilde{i}^2 r_i^2 k e^k I_1(k) \frac{B^2(r_i)}{2\mu_0} . \qquad (45)$$

The mean pressure exerted by the N coils on a support cylinder with radius $r_i$ and height $2z_0$ is given by

$$k_r = \frac{N K_r}{2\pi r_i 2 z_0} = \frac{B^2(r_i)}{2\mu_0} . \qquad (46)$$

The tension T in one D-turn is constant along the contour and follows from (8) to be

$$T = \frac{1}{2} k I B(r_i) r_i . \qquad (47)$$

With I from (40) inserted in (47) we get

$$T = \frac{1}{N} 2 k \tilde{i} r_i^2 \frac{B^2(r_i)}{2\mu_0} . \qquad (48)$$

## 3. Comparison of analytically and numerically calculated values of the inductances of D-coils

The formula (42) for the inductance $L_D$ of a D-coil was derived by disregarding the deviations from the 1/r-variation of the magnetic induction produced by the finite number of coils. To get an idea of the influence of this finite number, the inductance $L_{D,num}$ of a toroidal arrangement of N filamentary D-windings was calculated numerically with the computer program from [2]. Figure 10 shows $L_{D,num}$ normalized to $L_D$ according to (42) for a typical case: $A_m = 1.62$, corresponding to $k = 0,72$ or $r_a/r_i = 4.22$.

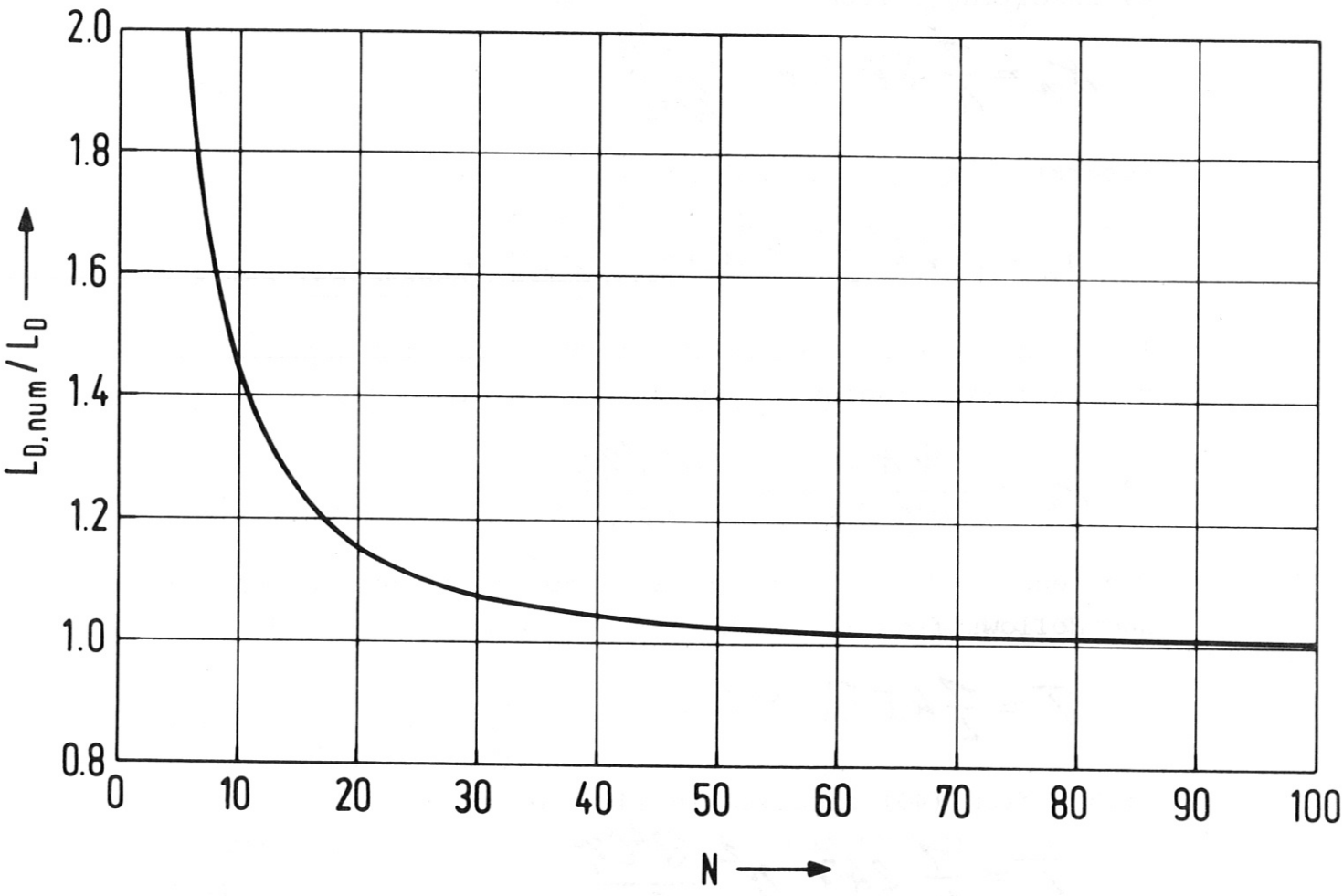


Fig. 10

## 4. Comparison of the stored magnetic energies in different types of elongated coils

The following results all pertain to ideal coils.

We shall replace the more academic parameter

$$k = \frac{\pi}{2} \ln (r_a / r_i) \tag{49}$$

by a "magnetic aspect ratio" $A_m$, which we define by

$$A_m = \frac{r_a + r_i}{r_a - r_i} . \tag{50}$$

For coils with circular minor cross-section $A_m$ reduces to $A_m = R/r$ (R and r are the major and minor radii respectively).

From (49) and (50) we get

$$A_m = \frac{\pi}{\tanh k} . \tag{61}$$

Eq, (51) and the approximation $A_m \approx 1/k$ are shown in Fig. 11.

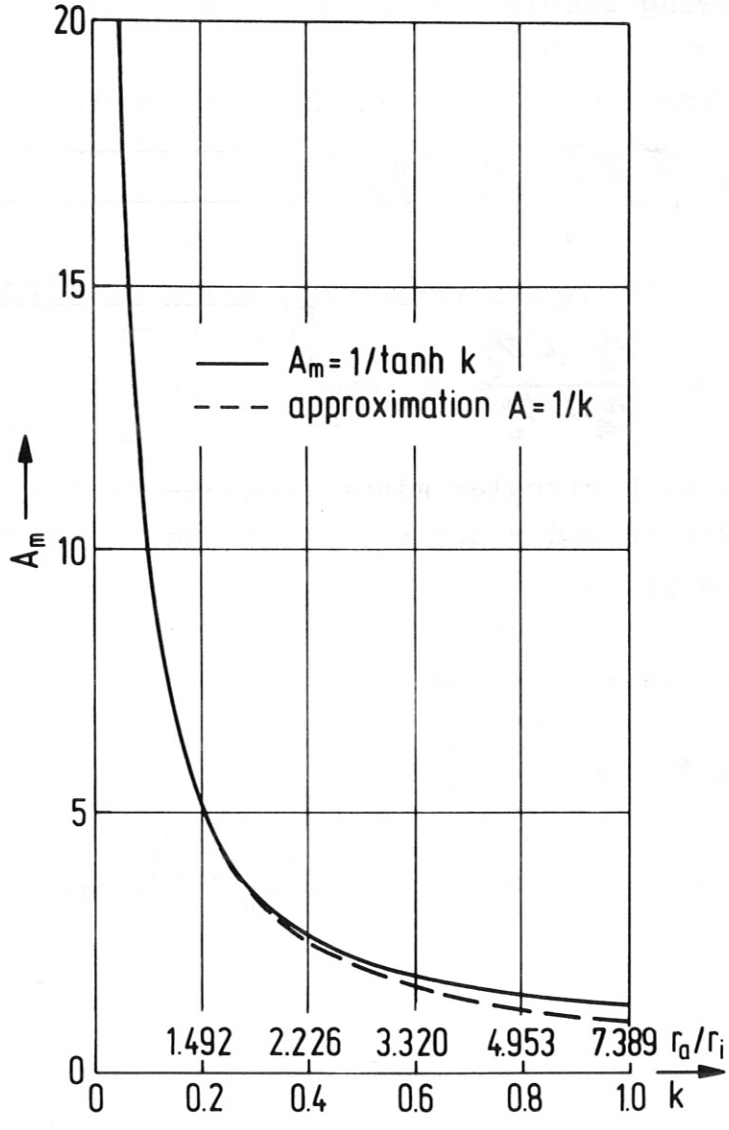
20
15
10
5
0
$A_m$
$A_m = 1/\tanh k$
approximation $A = 1/k$
1.492
2.226
3.320
4.953
7.389
$r_a/r_i$
0
0.2
0.4
0.6
0.8
1.0
k

Fig. 11

## 4.1 Rectangular coils

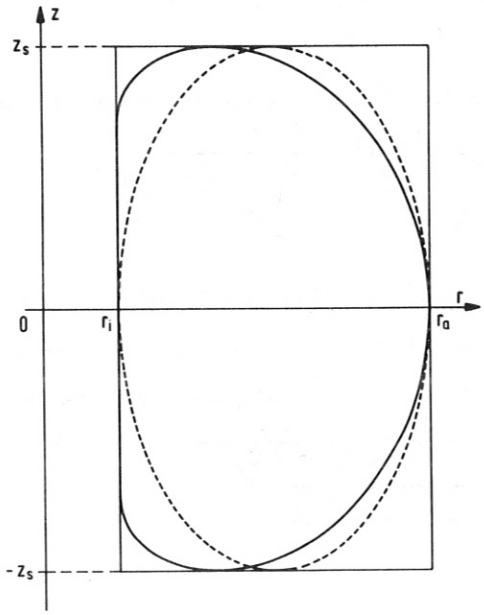


Fig. 12

By using (33) together with (34) and (1) we get for the magnetic energy $E_{m,r}$ stored in a rectangular coil (see Fig. 12):

$$E_{m,r} = \delta \tilde{r} 4 \frac{B^2(r_i)}{2\mu_0} r_i^2 z_s \,. \tag{52}$$

## 4.2 Elliptic coils

We now consider the elliptic coil inscribed into the rectangle in Fig. 12 (major axis = 2 $z_s$, minor axis = = $r_a - r_i$).

The stored magnetic energy $E_{m,e}$ can be calculated from $E_{m,c}$ for the circular coil as given by (38). We get for $E_{m,e}$

$$E_{m,e} = E_{m,c} \cdot \frac{2 z_s}{r_a - r_i} \quad . \tag{53}$$

After some rearrangement we find from (38) and (53)

$$E_{m,e} = \delta \bar{r}^2 \frac{(\sinh k/2)^2}{\sinh k} \cdot \frac{B^2(r_i)}{2\mu_0} r_i^2 z_s \quad . \tag{54}$$

The ratio of the magnetic energies stored in an elliptic coil and the corresponding rectangular coil (identical values of $r_i$, $z_s$ and $B(r_i)$ assumed) is given by

$$\frac{E_{m,e}}{E_{m,r}} = \frac{\pi}{4} \frac{(\sinh k/2)^2}{k \sinh k} \tag{55}$$

or

$$\frac{E_{m,e}}{E_{m,r}} = \frac{\pi}{2} \cdot \frac{A_m}{\operatorname{arctanh}(1/A_m)} \left(1 - \sqrt{1 - 1/A_m^2}\right) . \tag{56}$$

For values $A_m \gg 1$ we find from (56)

$$\frac{E_{m,e}}{E_{m,r}} \approx \frac{\pi}{4} = 0{,}7854 . \tag{57}$$

The curves corresponding to (56) and (57) are shown in Fig. 13 (two lower curves).

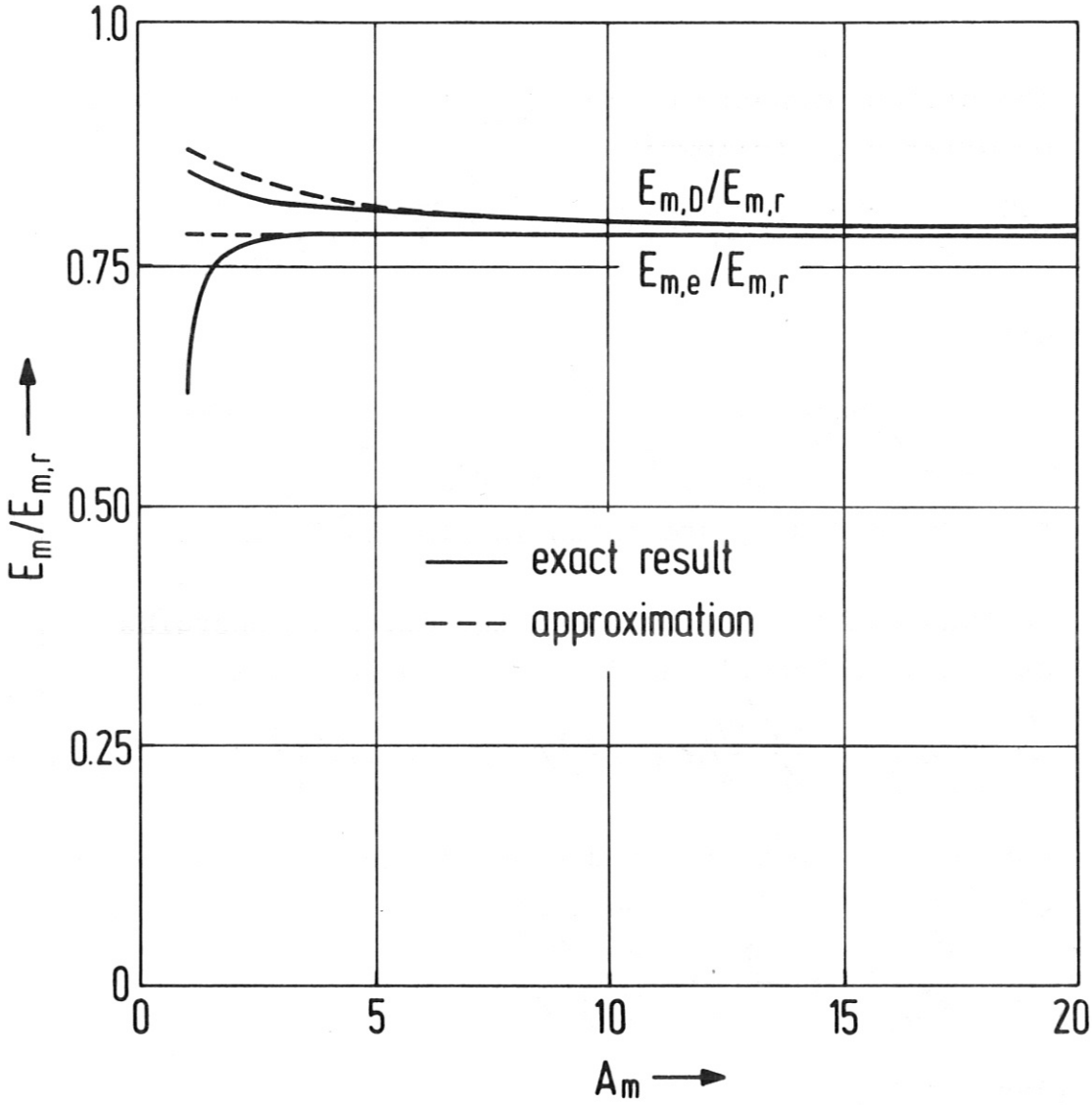


Fig. 13

## 4.3 D-coils

In contrast to rectangular and elliptic coils the values of $r_i$, $r_a$, and $z_s$ are interrelated for the case of D-coils. By selecting, for example, $r_a$ and $r_i$ we also fix $z_s$. This fact can be read from (32).

The stored magnetic energy $E_{m,D}$ according to (37) can be written as follows:

$$E_{m,D} = 4\pi^2 F(k)\left[kI_0(k) + (k-1)I_1(k)\right]\frac{B^2(r_i)}{2\mu_0} r_i^2 z_s \qquad (58)$$

with

$$F(k) = \frac{1}{\int_0^{\pi/2} e^{k\cos\alpha}\cos\alpha\, d\alpha} \,. \qquad (59)$$

F(k) vs. k and $A_m$ are shown in Fig. 14.

We thus get for the ratio of the magnetic energies stored in a D-coil and in a rectangular coil:

$$\frac{E_{m,D}}{E_{m,r}} = \frac{\pi}{2}\cdot\frac{F(k)}{k}\left[kI_0(k) + (k-1)I_1(k)\right]. \qquad (60)$$

For small values of k and hence large values of $A_m$ we get from (60), (59), and (51)

$$\frac{E_{m,D}}{E_{m,r}} \approx \frac{\pi}{4}\cdot\frac{1+k}{1+\pi/4\cdot k} \qquad (61)$$

(for $k \ll 1$) and

$$\frac{E_{m,D}}{E_{m,r}} \approx \frac{\pi}{4}\cdot\frac{A_m+1}{A_m+\pi/4} \qquad (62)$$

(for $A_m \gg 1$).

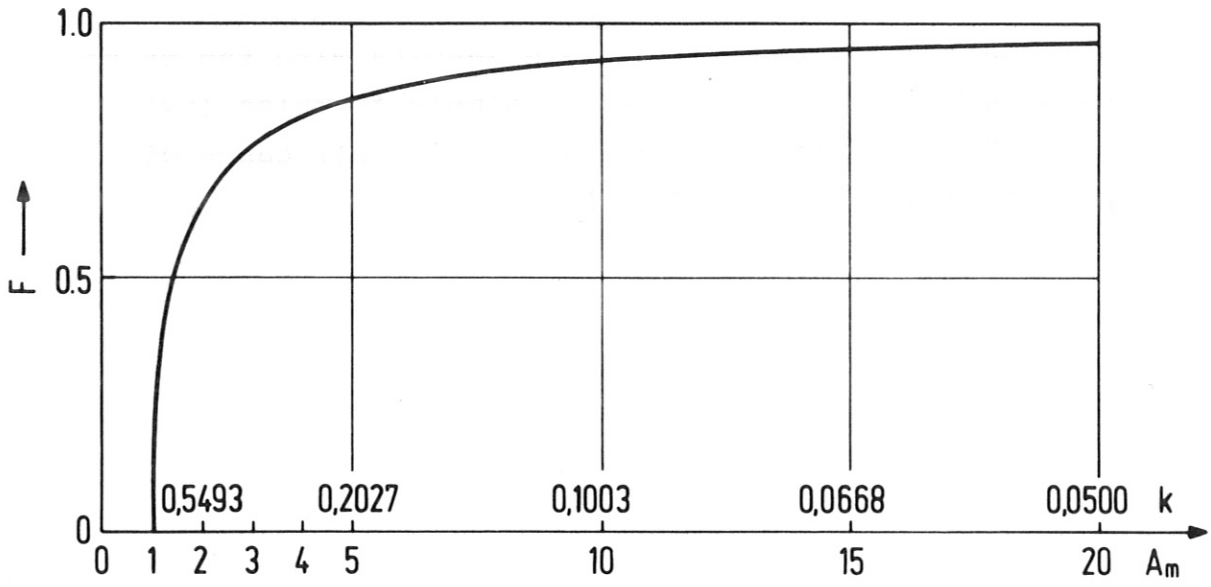


Fig. 14

Equations (60) and (62) are visualized in Fig. 13 (upper curves).

By comparing the stored magnetic energies in different types of elongated coils characterized by identical values of $r_i$ , $r_a$ , $z_s$ , and $B(r_i)$ we find

- the maximum energy is obviously stored in a rectangular coil,

- the magnetic energy in a D-coil is about 80 % of that in a rectangular one nearly independent of the aspect ratio $A_m$,

- the magnetic energy in an elliptical coil is only slightly smaller than that in a D-coil, the ratio of the two energies being nearly independent of $A_m$.

A comparison of the approximate results with the exact ones in Fig. 13 shows that the simple formulae (57) and (62) are sufficiently accurate for all cases of practical interest ($A_m \gtrsim 1.5$).

References

[1 ] J. File, R.G. Mills, G.V. Sheffield:
MATT 848, Princeton University, June 1971.

[2] H. Preis:
Calculation of the magnetic field, magnetic forces, and behaviour of large coil systems for fusion experiments,
IPP III/24, April 1976.